Plant Physiol. (1996) 110: 903–912

Determining Photosynthetic Parameters from Leaf CO_2 Exchange and Chlorophyll Fluorescence[1]

Ribulose-1,5-Bisphosphate Carboxylase/Oxygenase Specificity Factor, Dark Respiration in the Light, Excitation Distribution between Photosystems, Alternative Electron Transport Rate, and Mesophyll Diffusion Resistance

Agu Laisk* and Francesco Loreto

Tartu Ülikooli Molekulaar-ja Rakubioloogia Instituut, Riia tn. 181, Tartu, EE2400, Estonia (A.L.); and Istituto di Biochimica ed Ecofisiologia Vegetali, 00016 Monterotondo Scalo, Rome, Italy (F.L.)

Using simultaneous measurements of leaf gas exchange and chlorophyll fluorescence, we determined the excitation partitioning to photosystem II (PSII), the CO_2/O_2 specificity of ribulose-1,5-bisphosphate carboxylase/oxygenase, the dark respiration in the light, and the alternative electron transport rate to acceptors other than bisphosphoglycerate, and the transport resistance for CO_2 in the mesophyll cells for individual leaves of herbaceous and tree species. The specificity of ribulose-1,5-bisphosphate carboxylase/oxygenase for CO_2 was determined from the slope of the O_2 dependence of the CO_2 compensation point between 1.5 and 21% O_2. Its value, on the basis of dissolved CO_2 and O_2 concentrations at 25.5°C, varied between 86 and 89. Dark respiration in the light, estimated from the difference between the CO_2 compensation point and the CO_2 photocompensation point, was about 20 to 50% of the respiration rate in the dark. The excitation distribution to PSII was estimated from the extrapolation of the dependence of the PSII quantum yield on F/F_m to $F = 0$, where F is steady-state and F_m is pulse-saturated fluorescence, and varied between 0.45 and 0.6. The alternative electron transport rate was found as the difference between the electron transport rates calculated from fluorescence and from gas exchange, and at low CO_2 concentrations and 10 to 21% O_2, it was 25 to 30% of the maximum electron transport. The calculated mesophyll diffusion resistance accounted for about 20 to 30% of the total mesophyll resistance, which also includes carboxylation resistance. Whole-leaf photosynthesis is limited by gas phase, mesophyll diffusion, and carboxylation resistances in nearly the same proportion in both herbaceous species and trees.

Both gas-exchange and fluorescence measurements may be used to calculate the ETR (von Caemmerer and Farquhar, 1981; Genty et al., 1989). The difference between the ETR calculated from fluorescence and that calculated from gas-exchange measurements has been used to estimate the CO_2/O_2 specificity of Rubisco (Peterson, 1989, 1990), the mesophyll diffusion resistance and the chloroplastic CO_2 concentration (Di Marco et al., 1990; Loreto et al., 1992, 1994; Epron et al., 1995), the alternative electron sinks (Loreto et al., 1994), and the nonphotosynthetic carboxylation and decarboxylation rates (Laisk and Sumberg, 1994).

To calculate J_f and J_p (for denotations, see "Theory") each variable included in the respective equations must be correctly known. Accurate estimates of J_f depend on (a) the validity of the equation applied to find J_f from $\Delta F/F_m$ (Genty et al., 1989) and (b) the excitation distribution between PSI and PSII. Although the parameter $\Delta F/F_m$ has generally been found to be linearly related to the quantum yield of CO_2 fixation, nonlinear relationships between the two have also been reported (Seaton and Walker, 1990; Öquist and Chow, 1992). Excitation has usually been assumed to be equally distributed between PSI and PSII (Krall and Edwards, 1992; Loreto et al., 1992, 1994). Accurate estimates of J_p depend on (a) the CO_2/O_2 specificity of Rubisco, which determines the CO_2 photocompensation point at which photosynthesis and photorespiration are equal (on a CO_2 basis); (b) the rate of dark respiration in the light, which has to be subtracted from the total respiration to determine photorespiration; and (c) the mesophyll diffusion resistance, which lowers the CO_2 concentration at Rubisco active sites from that in the intercellular spaces, thus favoring oxygenation over carboxylation.

In principle, J_f and J_p may not be equal, since part of J_f may be used to reduce alternative acceptors, such as nitrite and O_2 (Badger, 1985; Robinson, 1988). Loreto et al. (1994) suggested that alternative electron sinks are generally too low to be detected under ambient conditions but found a residual electron transport of about 40 μmol m^{-2} s^{-1} when photosynthesis and photorespiration were selectively inhibited. If alternative electron sinks are relatively active, then the estimation of the mesophyll diffusion resistance from electron transport is not accurate. In previous works (Di Marco et al., 1990; Loreto et al., 1992, 1994; Laisk and Sumberg, 1994) some of these parameters were assumed to be constant (Rubisco specificity, dark respiration in the

[1] The work in Italy was supported by Consiglio Nazionale delle Ricerche-North Atlantic Treaty Organization Guest Fellowship No. 217.27/1.06 and in Estonia by International Science Foundation grant LLK100 for A.L.

* Corresponding author; e-mail laisk@park.tartu.ee; fax 372–7–421187.

Abbreviation: ETR, electron transport rate.

light, excitation distribution between PSI and PSII), and the others were calculated. However, to solve a system with many unknown variables, at least the same number of independent measurements are necessary. The correct procedure is one that makes the influence of each variable on the result maximum in one measurement and less in the other measurements. We report a series of experiments that were designed to satisfy this mathematical requirement and allowed us to estimate the variables affecting J_f and J_p calculations. Although this considerably reduced the degree of freedom of the system, it is still difficult to calculate alternative electron sinks and mesophyll diffusion resistance independently because of the similar influence of these two variables on the calculated photosynthetic electron transport.

THEORY

We calculated the ETR and the mesophyll diffusion resistance from the following system of equations that describes the relationships among electron transport, ribulose-1,5-bisP carboxylation, and photorespiratory CO_2 evolution.

$$P = G - R_p - R_d, \quad (1)$$

$$R_p = \frac{G \times O_c}{2K_s \times C_c}, \quad (2)$$

$$J_p = 4G + nR_p, \quad (3)$$

$$C_w = C_0 - r_{gw}P, \quad (4)$$

$$C_c = C_0 - (r_{gw} + r_{md})P, \quad (5)$$

$$O_c = \beta_o O_a, \quad (6)$$

$$r_{gw} = 100 \times \beta_c \left[\frac{p_k}{RT_l} \times \frac{S}{2V} \times \left(1 - \frac{ES}{V}\right) \times \left(1 - 1.62\frac{W_{ik} - W_a}{1013}\right) + r_g\left(1 - 1.62\frac{W_{ik} - W_a}{2026}\right)\right], \quad (7)$$

$$C_0 = 1000 \times \beta_c \frac{Up_k}{RT_l}\left(1 - \frac{ES}{2V}\right)\left(1 - 1.62\frac{W_{ik} - W_a}{1013}\right), \quad (8)$$

$$\beta_c = \exp\left(\frac{401.0}{105.7 + t_l} - 3.252\right), \quad (9)$$

$$\beta_o = \exp\left(\frac{131.2}{72.9 + t_l} - 4.815\right). \quad (10)$$

Denotations used above and in the forthcoming are the following: C_0, equivalent reference (inlet) CO_2 concentration, reduced to liquid phase considering solubility (CO_2 and O_2 concentrations in μmol m^{-3}); C_c, CO_2 concentration at carboxylation sites (dissolved); C_w, cell-wall CO_2 concentration (dissolved); E, rate of transpiration (mmol cm^{-2} s^{-1} in Eqs. 7 and 8); F, steady-state fluorescence yield; F_m, pulse-saturated fluorescence yield; G, gross photosynthesis (carboxylation) rate (rates in μmol m^{-2} s^{-1}); J_a, alternative ETR; J_f, ETR calculated from fluorescence; J_p, ETR that supports photosynthetic CO_2 exchange; K_s, CO_2/O_2 specificity of Rubisco; L_d, diffusion length from evaporation sites to external air; n, number of electrons consumed per CO_2 photorespired; O_c, O_2 concentration (dissolved) in chloroplasts; P, net CO_2 exchange rate; p_k, pressure in the leaf chamber (mbar); Q, absorbed quantum flux density (μmol m^{-2} s^{-1}); R, gas constant (83.12 mbar mL K^{-1} mmol); R_d, dark respiration rate in the light; R_p, photorespiration rate; r_c, carboxylation resistance (resistances in s m^{-1}); r_g, the gas phase resistance for CO_2 diffusion as calculated from the transpiration rate; r_{gw}, diffusion resistance in gas phase from chamber inlet to cell walls (evaporation sites), reduced to liquid phase; r_m, total resistance for diffusion and carboxylation in the liquid phase of mesophyll cells; r_{md}, diffusion resistance in liquid phase from cell walls (evaporation sites) to carboxylation sites; r_t, total resistance; S, leaf area in the chamber (cm^2 in Eqs. 7 and 8); T_l, leaf temperature (K); t_l, leaf temperature (°C); U, CO_2 concentration in the gas entering the leaf chamber as measured by the absolute gas analyzer (μmol mol^{-1}); V, actual flow rate into the leaf chamber (mmol s^{-1}); W_a, mean water vapor pressure in the leaf chamber (mbar); W_{ik}, mean water vapor pressure at the mesophyll cells (mbar); Y_{II}, quantum yield of electron transport at PSII; Y_{IIm}, relative excitation distribution to PSII; β_c and β_o, solubilities of CO_2 and O_2, respectively (m^3 m^{-3}); Γ, CO_2 compensation point; Γ^*, CO_2 photocompensation point.

Data for the approximation of solubilities were averaged from the works of Kaye and Laby (1962) and Mistshenko and Ravdel (1965). Equation 7 considers the dilution of CO_2 by water vapor (Laisk, 1977) and the counterflow of water vapor on the diffusion of CO_2 through the stomata (Parkinson and Penman, 1970).

Thus, the system of resistances is the following:

$$r_t = r_{gw} + r_{md} + r_c. \quad (11)$$

To make it comparable with the liquid phase resistances, the gas phase resistance r_g was multiplied by the solubility of CO_2 to obtain r_{gw} (Eq. 7). The total mesophyll resistance r_m is defined as

$$r_m = r_{md} + r_c. \quad (12)$$

Substituting Equation 2 into Equations 1 and 3, we obtain

$$G = \frac{P + R_d}{\left(1 - \frac{O_c}{2K_sC_c}\right)} \quad (13)$$

and

$$J_p = 4G\left(1 + \frac{nO_c}{8K_sC_c}\right). \quad (14)$$

Substituting G from Equation 13 into Equation 14, we obtain

$$J_p = \frac{4(P + R_d)}{1 - \frac{O_c}{2K_sC_c}} \times \left(1 + \frac{nO_c}{8K_sC_c}\right). \quad (15)$$

Substituting C_c from Equation 5 into Equation 15 and carrying out the necessary transformations, r_{md} is expressed as

$$r_{md} = \frac{C_0}{P} + \frac{O_c}{2K_sP} \times \frac{n(P + R_d) + J_p}{4(P + R_d) - J_p} - r_{gw} \quad (16)$$

and

$$J_p = 4(P + R_d) \times \frac{2K_s[C_0 - (r_{gw} + r_{md})P] + nO_c/4}{2K_s[C_0 - (r_{gw} + r_{md})P] - O_c}. \quad (17)$$

From fluorescence, ETR J_f was calculated as

$$J_f = QY_{IIm}\left(1 - \frac{F}{F_m}\right). \quad (18)$$

J_p is related to J_f and to the alternative ETR J_a as follows:

$$J_a = J_f - J_p. \quad (19)$$

Application of these equations for finding r_{md} and J_a requires precise measurements of CO_2 exchange rate and fluorescence under well-defined concentrations of CO_2 and O_2 and the knowledge of K_s, R_d, and Y_{IIm}.

K_s was determined from the slope of the O_2 dependence of G using O_2 values of less than 21%, where the contribution to G by dark respiration is constant

$$K_s = \frac{\Delta O_c}{2\Delta\Gamma}. \quad (20)$$

R_d was calculated from the total mesophyll conductance (the slope of the P versus C_w plot) and the difference $\gamma - \Gamma^*$, as follows:

$$R_d = \left(\Gamma - \frac{O_c}{2K_s}\right) \times \frac{P}{C_w - \Gamma}, \quad (21)$$

where the second term in parentheses represents Γ^*.

Y_{II} was calculated with respect to Q as

$$Y_{II} = J_p/Q, \quad (22)$$

where J_p is from Equation 17.

MATERIALS AND METHODS

Cowpea (*Vigna unguiculata* [L.] Walp.) plants were grown in a greenhouse. Attached leaves of 30-d-old plants were used in experiments. Leaves of *Xanthium strumarium* L., *Tilia cordata* L., *Citrus sinensis* L., and *Ficus carica* L. were collected from plants growing in the area of Consiglio Nazionale delle Ricerche, near Rome, in June to July 1995. Sunflower (*Helianthus annuus* L.) leaves were collected from a local field.

Gas-Exchange and Fluorescence Measurements

A round leaf chamber (0.031 m in diameter, 0.003 m high) was used. Gas entered and exited through two thin slits with a flow rate of 1 L min^{-1}. Each slit occupied 90° of the perimeter. Gas flow was laminar. The upper side of the leaf was sealed with starch paste to the thermostated glass window. This increased the heat conductance between the leaf and thermostating water to 300 to 500 W m^{-2}. As a result the increase in leaf temperature did not exceed 0.5°C under illumination. The actual leaf temperature was calculated from the energy budget of the leaf (Laisk, 1977). Gas exchange only through the lower epidermis was measured. This might decrease the resulting stomatal conductance for amphistomatous leaves but avoided complications arising from mixing air streams that had passed over different leaf surfaces (Bertsch and Domes, 1969).

Air was pumped through the open system creating 200 kPa overpressure. The pressure was stabilized at 100 kPa by a pressure-reducing valve. A column of NaOH on the input of the pump reduced CO_2 concentration to a few parts per million. The flow rate of the CO_2-free air was set to 3.76 L min^{-1} with an SP-1622 flow controller (Matheson, East Rutherford, NJ). Downstream, the dewpoint of the gas was set to 15°C. Air containing 3% CO_2 flowed through a flow controller (maximum rate 10 mL min^{-1}) into the humidified, CO_2-free air. The gas flow was divided in a manifold to feed (a) the leaf chamber and then measurement cells of the water vapor and CO_2 analyzers (Binos, Leybold-Hereus, Germany), operated in differential mode; (b) reference cells of the differential gas analyzers; (c) a zero-check circuit; and (d) an absolute CO_2 analyzer (LI 6200; Li-Cor, Lincoln, NE). The differential H_2O and CO_2 IRGAs were connected in sequence and the dewpoint of the gas was set to 0°C before entering the CO_2 IRGA. The zero of the absolute IRGA was set with pure N_2, and the span was calibrated with a standard gas of 354 ppm CO_2 in N_2 (Caracciolo, Rome, Italy). The differential IRGA was calibrated against the absolute one by stopping the reference flow and changing the absolute CO_2 concentration. Because of the pressure change in the reference cell, a small shift of the reference line was induced during the calibration but did not influence the response to the difference in CO_2 concentration. The H_2O IRGA was calibrated in a similar way, changing the dewpoint of the main gas flow. The pressure at the manifold was stabilized by a manostat tube immersed 50 cm in water. Flow rates to each of the four circuits were set by constant resistances (pieces of gas chromatograph capillary tubing). The flow rate through the leaf chamber was measured with a mass flowmeter (Matheson), calibrated against a bubble flowmeter (The Mini-Buck Calibrator, A.P. Buck, Orlando, FL). The O_2 concentration in the gas was controlled by feeding N_2 (or O_2) to the input of the pump through a flow controller. The tube carrying N_2 (O_2) from the flow controller was placed loosely in the pump inlet tube so that the pump captured all of the gas coming from the pressure cylinder and, if the flow rate from the cylinder was insufficient, the rest was taken from air. This arrangement avoided flow disturbances when changing the O_2 concentration and allowed us to obtain any O_2 concentration between 0 and 21% using a N_2 cylinder and between 21 and 100% using an O_2 cylinder.

The leaf chamber was illuminated through a light guide of plastic 1-mm-diameter fibers (Toray polymer optical fiber, PF-series; Laser Components, Gröbenzell, Munich, Germany) made in the University of Tartu (Estonia). By individual arrangement of each fiber, light from two

sources (KL 1500; Schott, Cologne, Germany) was evenly superimposed over the leaf area. Light was measured with an LI-185 quantum sensor (Li-Cor). Leaf absorbance was measured with the Li-Cor 1800 portable spectroradiometer and Li-Cor 1800-K integrating sphere. One KL 1500 provided 2-s pulses (10,000 μmol m^{-2} s^{-1}) for fluorescence saturation, and the other was used for actinic illumination. Light was attenuated with neutral filters mounted in the KL 1500 by the manufacturer. Using the same fiber arrangement, Chl fluorescence was measured from a 0.01- × 0.02-m^2 spot on the leaf with a PAM 101 fluorometer (Heinz-Walz, Effeltrich, Germany). Signals from the fluorometer and the differential IRGAs were recorded on a chart recorder.

Gas-Exchange Data Processing

In the laminar flow chamber, transport resistances to CO_2 were calculated with respect to the mean CO_2 concentration in the chamber, but for water vapor the program divided the leaf chamber into several small sections. Water vapor pressure at the output of a section served as the input for the next section. Leaf temperature was calculated separately for each section from the energy budget. Water vapor pressure in leaf intercellular spaces was assumed to be saturating at the leaf temperature and was calculated from the Magnus formula. For each section, transpiration rate was calculated on the basis of the water vapor pressure difference between the leaf intercellular air spaces and chamber air and the diffusion resistance. The latter was assumed to be the same for all sections and was expressed as L_d to exclude the influence of different diffusion coefficients in different gas mixtures. The increasing water vapor pressure was integrated over the chamber length, and L_d was iterated until the calculated water vapor pressure at the end of the chamber became equal to the measured value. The L_d that corresponded to this condition was used in further calculations of the diffusion resistances for CO_2. The average heat conductance between the leaf and the thermostating water was found by solving a system of energy budget equations for two transpiration measurements carried out at different light intensities at constant stomatal opening (readings of transpiration were taken before the stomatal movements commenced).

A second loop of iteration was placed over the iteration of L_d and was continued with plausible heat-exchange coefficients until the L_ds calculated for both transpiration rates were the same. The value of the heat-exchange coefficient that satisfied this condition was used for the calculations of L_d for gas-exchange measurements. The equivalent gas phase resistance for CO_2 (r_{gw}, Eq. 7), which accounts also for the "chamber resistance," S/V, dilution of the CO_2 by water vapor, and the effect of the viscous flow of water vapor out from the leaf (Parkinson and Penman, 1970), was calculated. To make gas phase and liquid phase resistances comparable, the gas phase resistance was multiplied by the CO_2 solubility. Similarly, C_0 (Eq. 8) was calculated from the reading of LI-6200. The average water vapor pressure on the diffusion path of CO_2 was considered, and the concentration was multiplied by the CO_2 solubility to compare concentrations in gas and liquid phases. Thus, the corrections considered in the calculation program were the influences of atmospheric pressure, temperature, and gas molecular weight (different $O_2/N_2/H_2O$ ratios) on the flow rate through the leaf chamber, the increase of the flow rate due to transpiration, the dilution of the CO_2 concentration due to higher water vapor pressure in the intercellular air space, and the effect of viscous counterflow of water vapor from the leaf on CO_2 diffusion into the leaf (Laisk, 1977). When these corrections are included in r_{gw} and C_0 (Eqs. 7 and 8), the calculation of C_w is as simple as Equation 4.

RESULTS

CO_2/O_2 Specificity of Rubisco and Dark Respiration in the Light

K_s was calculated from the slope of the O_2 dependence of Γ (CO_2 concentration at which photosynthesis equals total respiration in the light). We made the assumption that R_d was independent of O_2 concentration over the used range. At low O_2 concentrations (between 1.5 and 21%), the slope of the P versus C_w curves near Γ little depends on the O_2 concentration (Fig. 1) and, thus, the difference $\Gamma - \Gamma^*$ stays constant. Therefore, we can express K_s, replacing $\Delta\Gamma$ for Γ^* and ΔO_c for O_c (Eq. 20).

To measure Γ, the open system was tuned to different CO_2 concentrations, one somewhat below and the other a little above Γ, and Γ was found by linear interpolation. Net CO_2 exchange rates of a sunflower leaf measured at different CO_2 and O_2 concentrations are plotted against C_w in Figure 1. The dependence of Γ on O_c for O_2 concentrations between 1.5 and 100% for the same leaf is shown in Figure 2. The slope of the dependence stays constant below O_c of 0.262 mol m^{-3} (21%). The line intercepts the axis of Γ very close to 0, and the slope slightly increases only at higher O_2 concentrations, indicating that the contribution of R_d to Γ is small. Values for K_s, calculated from the slope of the Γ

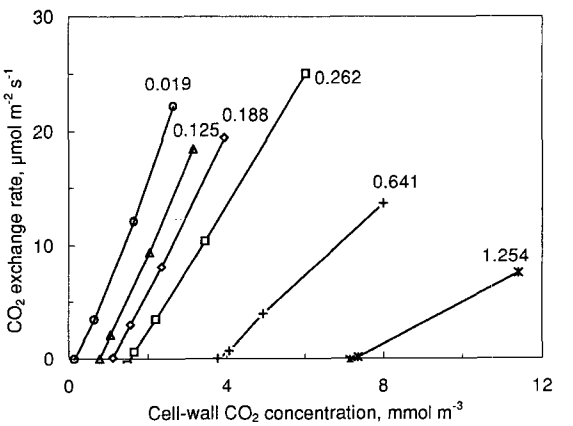

Figure 1. CO_2 exchange rate of a *Helianthus* leaf as a function of the calculated cell-wall (dissolved) CO_2 concentration. Different curves were measured at O_2 concentrations labeled at the curves in mol m^{-3}. Q = 1110 μmol m^{-2} s^{-1}; t_l = 25.5°C.

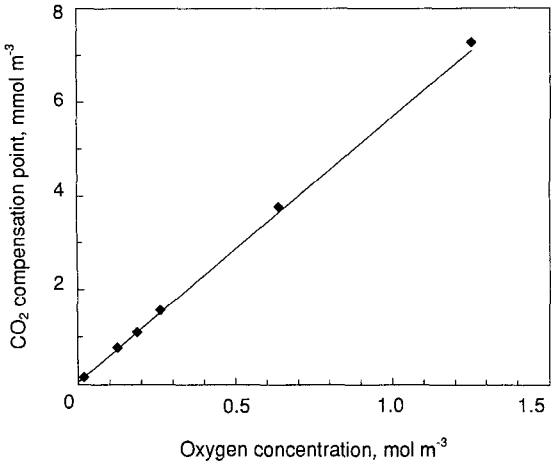

Figure 2. Dependence of the CO_2 compensation point on dissolved O_2 concentration for *Helianthus* (data from Fig. 1).

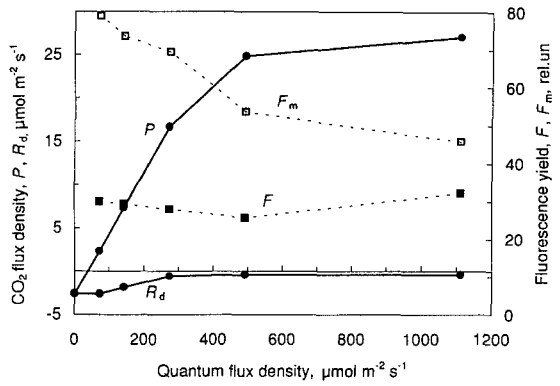

Figure 3. Light curves of CO_2 exchange rate (P) and dark respiration in the light (R_d) (solid lines, left axis) and steady-state (F) and pulse-saturated (F_m) fluorescence yields (dashed lines, right axis) for *Helianthus* at 1.5% (0.019 mol m^{-3}) O_2 and external CO_2 concentration of 196 ppm (C_0 = 6600 μmol m^{-3}). R_d was determined as described in the text. rel.un, Relative units.

versus O_c dependence between 1.5 and 21% O_2 are given in Table I for different plants. If K_s is known, it is possible to calculate R_d from the total mesophyll conductance (the slope of the P versus C_w plot) and the difference $\Gamma - \Gamma^*$ (Eq. 21). The calculated dark respiration in the light (Table I) was relatively low, about 20 to 50% of the value in the dark.

Excitation Distribution to PSII and Electron Transport to Alternative Acceptors

To correctly calculate the ETR from Equation 18 we need to know Y_{IIm}. It was determined from the relationship between photosynthesis and Chl fluorescence when photorespiration was suppressed by decreasing O_2 concentration to 1.5%. Stable photosynthetic rates were measured sequentially at five values of Q and in the dark (Fig. 3). At each Q, F was recorded and one saturation pulse was given. To obtain data points at very low quantum yields, CO_2 concentration was decreased at the maximum Q. J_P was calculated from the measured gas-exchange rate using Equation 17, considering the presence of photorespiration in 1.5% O_2. Y_{II} was calculated according to Equation 22 and plotted against F/F_m (Fig. 4). This plot is the graphic representation of Equation 18 and yields a straight line that extrapolates to 0 when F approaches F_m and to Y_{IIm}, the maximum quantum yield of PSII, when F approaches 0. The parameter Y_{IIm} is the excitation distribution factor to PSII. Note that in Equation 22 Y_{II} is defined with respect to the total absorbed quanta, to find its value as excitation distribution factor to PSII when F approaches 0.

The placement of data points in the plot in Figure 4 depends on an assumption about how the dark respiration is inhibited with increasing light intensity. Assuming that the dark respiration was inhibited with increasing Q as shown in Figure 3, the points obtained at nonsaturating Q were placed close to a straight line. Since gradual inhibition of dark respiration in parallel with the light saturation of photosynthesis is possible, our data do not disagree with a linear Y_{II} versus F/F_m relationship. Experimental points obtained at saturating Q and lower CO_2 concentrations extrapolated to F/F_m values below 1. We interpret this as evidence of an alternative, nonphotosynthetic electron flow, which makes ETR calculated from gas-exchange mea-

Table I. *Photosynthesis parameters of individual leaves, as determined from the measurements of CO_2 exchange and Chl fluorescence*

K_s, the CO_2/O_2 specificity of Rubisco; Y_{IIm}, the excitation distribution to PS II; R_d, the dark respiration rate in the light; J_{fmax}, the maximum electron transport rate under photorespiratory conditions; J_{amax}, the maximum alternative electron transport; r_m, the mesophyll resistance (carboxylation plus diffusion); r_{md}, the mesophyll diffusion resistance; r_{mdmax}, the maximum r_{md} calculated with J_a = 0; r_{gw}, the gas phase resistance for CO_2 diffusion.

Species	K_s	Y_{IIm}	R_d	J_{fmax}	J_{amax}	r_m	r_{md}	r_{mdmax}	r_{gw}	r_{md}/r_m
	unitless			*µmol m^{-2} s^{-1}*			*s m^{-1}*			*unitless*
Helianthus	88.9	0.46	0.46	272	61.5	160	39.7	70.7	167	0.25
Xanthium	86.5	0.52	0.50	234	57.4	208	60.0	98.4	154	0.29
Vigna	86.2	0.48	0.25	168	18.2	233	22.9	50.0	307	0.10
Vigna	88.5	0.46	0.29	173	41.5	212	22.4	71.2	237	0.11
Vigna	85.8	0.42	0.34	134	24.1	277	40.0	91.0	317	0.14
Tilia	90.26	0.60	0.0	161	24.0	284	79.5	124	295	0.28
Ficus	89.6	0.57	0.28	142	12.1	320	37.4	79.0	239	0.12
Citrus	85.8	0.57	0.46	116	20.3	413	88.5	156	440	0.21
Citrus	85.8	0.58	0.278	75	13.7	548	100	184	444	0.18

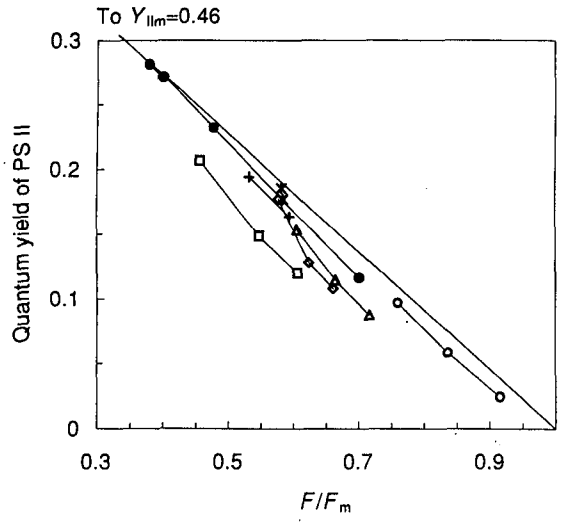

Figure 4. Quantum yield of electron transport as a function of the ratio F/F_m for *Helianthus*. Data points represent the quantum yield of photosynthetic electron transport, J_p/Q, calculated with the mesophyll diffusion resistance, r_{md}, of 39.7 s m^{-1}. Different series were measured at different O_2 concentrations by changing CO_2 concentration (symbols as in Fig. 1). Filled circles were obtained by decreasing light (as in Fig. 3). Straight line to $F/F_m = 1$ is the quantum yield of PSII electron transport, J_f/Q, calculated from Equation 18 with $Y_{IIm} = 0.46$.

surements lower than ETR calculated from fluorescence measurements.

The difference between J_f and J_p was even more evident from measurements at O_2 concentrations higher than 1.5% (Fig. 4). For these data, J_a was calculated from Equation 19 substituting J_p from Equation 17 and J_f from Equation 18. Results for *Helianthus* are shown in Figure 5. Three data points were measured at each O_2 concentration, as shown in Figure 1 (data that are close to the CO_2 compensation point cannot be used in these calculations). J_a generally decreased with increasing CO_2 concentration and increased with increasing O_2 concentration below 21% (0.262 mol m^{-3}) but decreased at higher O_2 concentrations. A similar O_2 and CO_2 dependence of J_a was obtained for *Xanthium* and *Vigna*. Tree species having lower ETR than herbaceous species did not show a clear CO_2 and O_2 dependence of J_a. Maximum J_f and maximum J_a for each experimental leaf are given in Table I.

Mesophyll Diffusion Resistance

The reciprocal of the P versus C_w slopes (Fig. 1) is r_m (Eq. 12). Since r_{md} is not influenced by the O_2 concentration (Loreto et al., 1992), the reduction of the slopes of the P versus C_w curves at high O_2 concentrations in Figure 1 indicates an increase in r_c. For the most correct evaluation of r_{md}, r_c must be kept to a minimum. This condition is met at O_2 concentrations below 21%. On the other hand, fast electron consumption by photorespiration is necessary to correctly calculate r_{md}. This occurs at high O_2 concentrations. Thus, the optimum range of O_2 concentrations for the evaluation of r_{md} seems to be between 10 and 21% O_2, where R_p is sufficiently high but r_c has not yet begun to increase.

The r_{md} was calculated from Equation 16 using J_p from Equation 17 and K_s, R_d, Y_{IIm}, and J_a values determined as described above. The average values of r_{md} from measurements at O_2 concentrations of 10, 15, and 21% are given in Table I. As seen from Equations 16, 17, and 19, J_a and r_{md} are interdependent and cannot be resolved in the framework of our data without applying assumptions. Maximum r_{md} in Table I was calculated assuming that $J_a = 0$ at any combination of CO_2 and O_2 concentrations, to show the possible range of variation of r_{md}. Another quite likely r_{md} value was chosen that resulted in $J_a = 0$ at only one pair of CO_2 and O_2 concentrations but $J_a > 0$ at others. For example, data in Figures 4 and 5 were calculated assuming that $r_{md} = 39.7$ s m^{-1}. Data from Table I are illustrated by Figure 6, where r_c, r_{md} calculated with and without J_a, and r_{gw} are shown. The last resistance may be somewhat overestimated for amphistomatous leaves, since diffusion through the stomata of the upper epidermis was blocked in our leaf chamber. The limiting role of each of these resistances is represented by its portion of the total.

DISCUSSION

This work shows that simultaneous fluorescence and gas-exchange measurements can be used to resolve the parameters involved in the current model of photosynthetic electron transport, CO_2 assimilation, and photorespiration. To do this, a system of experiments is proposed that allowed us to determine the Rubisco specificity factor, dark respiration in the light, excitation distribution to PSII, alternative electron transport to nonphotosynthetic acceptors, and mesophyll diffusion resistance. These parameters are necessary to calculate the electron transport, carboxylation (photosynthesis), and oxygenation (photorespira-

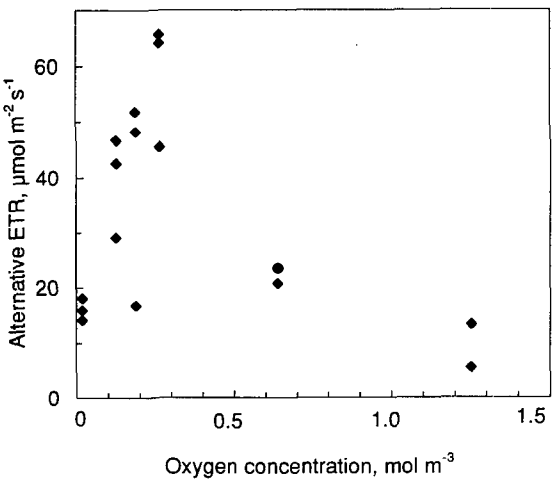

Figure 5. Dependence of J_a on O_2 and CO_2 concentrations for *Helianthus*. J_a was calculated from the difference between the data points of J_p/Q and the straight line of J_f/Q in Figure 4. Lower data points at each O_2 concentration correspond to higher CO_2 concentrations.

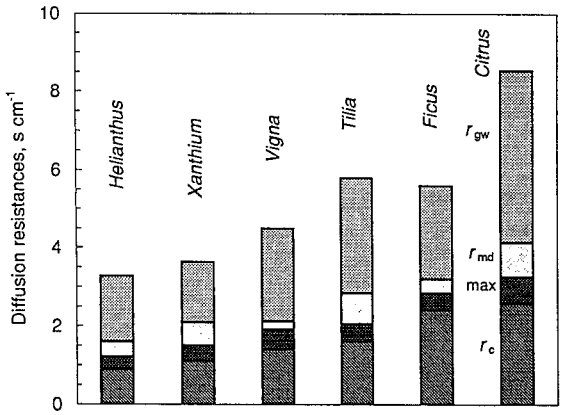

Figure 6. Resistances for carboxylation, r_c (bottom bar), for diffusion in gas phase to cell walls (evaporation sites), r_{gw} (top bar), and for diffusion from cell walls (evaporation sites) to carboxylation sites, r_{md} (the lightest bar). The dark area (max) between r_c and r_{md} shows the maximum possible extension of r_{md} if alternative electron transport is assumed to be absent.

tion) rates at different CO_2 and O_2 concentrations and light intensities.

Theoretical cornerstones of this work are (a) that CO_2 and O_2 competition for ribulose-1,5-bisP at Rubisco is quantitatively described correctly and (b) that fluorescence from the PSII pigments is quantitatively related to electron transport. The competition of CO_2 and O_2 for ribulose-1,5-bisP (Laisk, 1970; Ogren and Bowes, 1971; Laisk and Oja, 1972) is widely accepted and has been used for the description of the relationships between photosynthesis and photorespiration (Farquhar and von Caemmerer, 1982). Some discrepancies between experiments and theory (Bravdo and Canvin, 1979; Pärnik, 1985; Hanson and Peterson, 1985) can be explained by the existence of alternative, nonphotosynthetic carboxylation and decarboxylation, which become dominant when photorespiration is suppressed at high CO_2 concentrations (Laisk and Sumberg, 1994). At limiting CO_2 concentrations, only a small residual dark respiration may interfere with the photosynthetic and photorespiratory CO_2 fluxes. We carefully checked the O_2 dependence of the CO_2 compensation point, a major consequence of the competition between the two gases, and found it to be linear, as required by the theory. In intact leaves, K_s has been calculated from Γ^* (the CO_2 concentration at which photosynthesis and photorespiration equilibrate, Laisk, 1970, 1977), previously determined from the mutual interception of the CO_2 curves of photosynthesis measured at different light intensities (Laisk and Oja, 1972; Laisk, 1977; Brooks and Farquhar, 1985). This is a cumbersome procedure that may underestimate Γ^*. As suggested by Sumberg and Laisk (1996), we determined K_s from the slope of the O_2 dependence of Γ at low O_2 concentrations, where the contribution of the dark respiration to the difference $\Gamma - \Gamma^*$ was constant. K_s, expressed with respect to dissolved gas concentrations at 25.5°C, varied from 86 to 90. This is in good agreement with in vitro measurements (Jordan and Ogren, 1984; Kane et al., 1994), also closely comparable with the K_s of 94 for spinach obtained in leaves by determining Γ^* from the measurements at different CO_2 concentrations and light intensities (Brooks and Farquhar, 1985). With a method based on the comparison of fluorescence and gas-exchange measurements, Peterson (1990) calculated similar K_s values for tobacco. The dependence of K_s on irradiance in the latter study was probably caused by inadequate consideration of J_a. With this K_s, dark respiration in the light, calculated from the difference of Γ and Γ^*, was about 20 to 30% of the dark value. Suppression of the respiratory CO_2 evolution in the light may be caused by the competition between reducing equivalents produced from photorespiration and those produced from the Krebs cycle, but it does not necessarily mean that O_2 uptake by mitochondria should decrease in the light.

This question is related to the number of electrons consumed per CO_2 photorespired, n. We did the calculations assuming that $n = 8$, as was done in previous works (Harley et al., 1992; Edwards and Baker, 1993; Epron et al., 1995). In fact, six electrons are required to reduce the three phosphoglyceraldehydes produced after the evolution of one CO_2. In addition, two electrons are required to reassimilate the NH_3. It is still subject to discussion whether the reducing equivalents produced in mitochondria at the Gly-Ser conversion are shuttled to peroxisomes for the reduction of hydroxypyruvate. If some of these reducing equivalents are oxidized to produce ATP in mitochondria, an equivalent amount should be drained from the photosynthetic electron transport chain for the reduction of hydroxypyruvate. As a matter of fact, the suppression of the CO_2 evolution from the Krebs cycle in the light may lead to the drainage of an equivalent amount of electrons to mitochondria from the photosynthetic electron transport chain. Therefore, $n = 8$ or probably even somewhat greater. Increase of n for one in the calculations somewhat decreased the calculated mesophyll diffusion resistances r_{md} but did not alter qualitative conclusions.

The interpretation of fluorescence is still problematic. The simple relationship between PSII electron transport and fluorescence used here is based on the physical model of competition among photochemical, thermal, and fluorescent de-excitations (Butler and Kitajima, 1975), from which Equation 18 was derived and experimentally checked under nonphotorespiratory and photorespiratory conditions (Genty et al., 1989, 1992). However, this relationship does not hold under low light intensities (Seaton and Walker, 1990; Öquist and Chow, 1992). Because of this, the quantitative interpretation of the fluorescence signal, especially in its long-wave shoulder as measured by the pulse amplitude modulation fluorometer, is controversial. We found that at low-photorespiratory conditions over wide ranges of light intensities, the agreement between experimental data and Equation 18 was good, provided that dark respiration was suppressed in the light and a small alternative electron transport J_a was assumed at high light intensities. One argument against the leaf fluorescence measurements has been the optical thickness that makes fluorescence from the upper parenchyma layers dominant (Loreto et al., 1994). This seems not to be a

problem, probably because the pulse amplitude modulation instrument measures mostly the long-wave shoulder of fluorescence, where leaf absorption decreases. It must also be considered that the photosynthetic activity of the leaf mesophyll cells is adapted to the average light intensity in that mesophyll layer (Laisk and Oja, 1976), because the relative degree of light saturation of photosynthesis is almost the same in all mesophyll cells independent of their location. Probably the best evidence to support the above considerations has been given by Edwards and Baker (1993), who found equally good correlation between ETRs derived from fluorescence and gas exchange whether fluorescence was monitored from the upper or from the lower side of the leaf. In the long-wave shoulder some fluorescence may come from PSI even at room temperature (Genty et al., 1990). We made calculations with 30% reduced dark fluorescence, but this yielded a slightly nonlinear relationship between Y_{II} and F/F_m (Loreto et al., 1994).

The extrapolation of the relationship of Y_{II} versus F/F_m to $F = 0$ yielded a maximum value Y_{IIm} that may be interpreted as excitation distribution factor to PSII. In most previous studies, this factor has been assumed equal to 0.5 (Loreto et al., 1992, 1994; Brestic et al., 1995). Y_{IIm} is in fact close to 0.5 but in our measurements still varied from 0.42 to 0.6 (Table I). The lower Y_{IIm} values were obtained from leaves exposed to high light in their natural habitats. In tree leaves, Y_{IIm} was higher, probably because these leaves were collected from partially shaded sites. Since fluorescence losses are inevitable in energy transfer to PSII, but fluorescence is very low from PSI, it is possible that shaded leaves maximize the total quantum yield of photosynthesis by distributing more light to PSII. For example, in *Tilia*, *Ficus*, and *Citrus*, PSII absorbed 60% of quanta but was able to efficiently use only about 40%, whereas PSI then absorbed 40% and was probably able to efficiently use all by maintaining 100% reduction of P700. As a result, only 20% of total quanta was lost. If excitation were equally distributed, both photosystems would work at 67% efficiency: PSII because of fluorescence losses and PSI because of limited electron supply resulting in oxidation of P700. The lower Y_{IIm} may also be one of the symptoms of photoinhibition.

The alternative electron transport to nonphotosynthetic acceptors probably represents fluxes to nitrite and O_2 photoreduction (Robinson, 1988). The first of them is small, probably even less than that observed at an O_2 concentration of 1.5% (Fig. 5). Since we found the alternative flux increasing with O_2 concentration, we suggest that it reflects the Mehler-type O_2 reduction at the acceptor side of PSI (Badger, 1985). Half of it then is the electron flux to form H_2O_2 and the other half is used to scavenge this dangerous compound through the Halliwell-Asada cycle (Foyer et al., 1994). This is supported by the fact that J_a increases with increasing of O_2 concentration only until electron transport is severely blocked at the acceptor side of PSI. When the electron pressure is released by higher CO_2 and O_2 concentrations at Rubisco, J_a decreases. Even the very high O_2 concentrations of 50 and 100% could not override the very low electron pressure and J_a still remained low. In plants with active alternative electron transport, such as *Helianthus*, *Vigna*, and *Xanthium*, J_a increased up to the atmospheric O_2 concentration, which shows that the apparent $K_m(O_2)$ of the process may be rather high. Still, these data must be interpreted with caution, since there is mutual interdependence among J_a, R_d, and r_{md}. If R_d were not constant, as assumed, but variable with CO_2 and O_2 concentrations, the O_2 dependence of J_a may be smaller than presented in Figure 5. The absolute values of J_a could not be precisely determined because of the above-mentioned interdependence. However, the values of J_a in Table I were obtained by choosing r_{md}, which did not yield negative J_a values at any experimental point, especially at higher CO_2 and O_2 concentrations where J_a was smaller. These values of J_a are consistently approximately 20 to 25% of the measured maximum ETR. Similar J_a values have been reported to occur in chloroplasts and protoplasts (Badger, 1985; Robinson, 1988) and in wheat leaves (Loreto et al., 1994) after the inhibition of the carbon reduction/oxidation cycle by glyceraldehyde. Measurements of alternative electron transport in leaves infiltrated with glyceraldehyde in the latter work indicated that residual electron transport was present when carbon metabolism was completely inhibited but could not reveal whether J_a was present in ambient conditions.

The presence of the alternative electron transport influences the calculation of mesophyll diffusion resistance. If the alternative electron transport is assumed to be absent, then the mesophyll diffusion resistance calculated from our experiments is comparable to those previously reported in the literature, both for trees that have high r_{md} (Lloyd et al., 1992; Loreto et al., 1992; Epron et al., 1995; Syvertsen et al., 1995) and for herbaceous species that have low r_{md} (Loreto et al., 1992, 1994; Evans et al., 1994; Laisk and Sumberg, 1994). This indicates that the total error made by assuming the specificity factor, the energy excitation partitioning to photosystems, and the dark respiration in the light as constants has a relatively small effect on the estimation of r_{md}. However, if J_a is considered, then the estimated r_{md} is reduced by about half in all species. These reduced r_{md} values are also comparable with those obtained by measuring the total discrimination against ^{13}C in photosynthesis (Evans et al., 1986; von Caemmerer and Evans, 1991). Therefore, the CO_2 concentration at the Rubisco sites may be higher than previously estimated, and photosynthesis may be limited by r_{md} to a lesser extent than previously considered, particularly in tree species (Epron et al., 1995). We found that the second component of mesophyll resistance (r_c), which is associated with carboxylation, is also higher in trees than in herbaceous species and is particularly high in the sclerophytic *Citrus* plants. Thus, the limitation to photosynthesis of the mesophyll cells in trees is mainly related to low Rubisco content or activity. The mesophyll diffusion resistances r_{md} obtained by us are about 3 times lower than the r_{md} calculated by Laisk et al. (1970) for some tree and herbaceous species on the basis of leaf anatomy. This means that either the average diffusion path length of CO_2 in the liquid phase is shorter than 1 μm, as was assumed in that work, or parallel diffusion of CO_2

and bicarbonate reduces the resistance. The latter model has recently been doubted (Price et al., 1994), since reduction of the expression of carbonic anhydrase did not result in increased mesophyll resistance in transgenic tobacco. Thus, the low diffusion resistance suggests that the actively functioning Rubisco is not spread in the whole stroma but is mainly concentrated in the part of the stroma close to the cell wall. Considering that a part of r_{md} obtained by our method may actually be in the gaseous phase of intercellular spaces (Parkhurst, 1994), the liquid phase resistance may be even smaller than our r_{md}. Whole-leaf photosynthesis is limited by gas phase, mesophyll diffusion, and carboxylation resistances in nearly the same proportion in trees and in herbaceous species.

ACKNOWLEDGMENTS

We thank Dr. Giorgio Di Marco for helpful discussions, advice, and care and Dr. Vello Oja for providing the program SYNTE.

Received August 11, 1995; accepted December 13, 1995.

LITERATURE CITED

Badger MR (1985) Photosynthetic oxygen exchange. Annu Rev Plant Physiol **36:** 27–53

Bertsch A, Domes W (1969) CO_2 Gaswechsel der amphistomatischer blätter. I. Der Einfluss unterschiedlicher Stomaverteilungen der beiden Blattepidermen auf den CO_2 transport. Planta **85:** 183–193

Bravdo BA, Canvin D (1979) Effect of carbon dioxide on photorespiration. Plant Physiol **63:** 399–401

Brestic M, Corric G, Fryer MJ, Baker NR (1995) Does photorespiration protect the photosynthetic apparatus in French bean leaves from photoinhibition during drought stress? Planta **196:** 450–457

Brooks A, Farquhar GD (1985) Effect of temperature on the CO_2/O_2 specificity of ribulose-1,5-bisphosphate carboxylase/oxygenase and the rate of respiration in the light. Planta **165:** 397–406

Butler WL, Kitajima WL (1975) Fluorescence quenching in photosystem 2 of chloroplasts. Biochim Biophys Acta **376:** 116–125

Di Marco G, Manes M, Tricoli D, Vitale E (1990) Fluorescence parameters measured concurrently with net photosynthesis to investigate chloroplastic CO_2 concentration in leaves of *Quercus ilex* L. J Plant Physiol **136:** 538–543

Edwards GE, Baker NR (1993) Can CO_2 assimilation in maize leaves be predicted accurately from chlorophyll fluorescence analysis? Photosynth Res **37:** 89–102

Epron D, Godard D, Cornic G, Genty B (1995) Limitation of net CO_2 assimilation rate by internal resistances to CO_2 transfer in the leaves of two tree species (*Fagus sylvatica* L. and *Castanea sativa* Mill.). Plant Cell Environ **18:** 43–51

Evans JR, Sharkey TD, Berry JA, Farquhar GD (1986) Carbon isotope discrimination measured concurrently with gas exchange to investigate CO_2 diffusion in leaves of higher plants. Aust J Plant Physiol **13:** 281–292

Evans JR, von Caemmerer S, Setchell BA, Hudson GS (1994) The relationship between CO_2 transfer conductance and leaf anatomy in transgenic tobacco with reduced content of Rubisco. Aust J Plant Physiol **21:** 475–495

Farquhar GD, von Caemmerer S (1982) Modelling of photosynthetic response to environmental conditions. *In* OL Lange, PS Nobel, CB Osmond, H Ziegler, eds, Physiological Plant Ecology. Encyclopedia of Plant Physiology, New Series, Vol 12B. Springer-Verlag, Berlin, pp 549–588

Foyer CH, Descourvieres P, Kunert KJ (1994) Protection against oxygen radicals: an important defence mechanism studied in transgenic plants. Plant Cell Environ **17:** 507–523

Genty B, Briantais JM, Baker NR (1989) The relationship between quantum yield of photosynthetic electron transport and quenching of chlorophyll fluorescence. Biochim Biophys Acta **990:** 87–92

Genty B, Goulas Y, Dimon B, Peltier G, Briantais JM, Moya I (1992) Modulation of efficiency of primary conversion in leaves: mechanisms involved at PS2. *In* N Murata, ed, Research in Photosynthesis, Vol IV. Kluwer Academic, Dordrecht, The Netherlands, pp 602–610

Genty B, Wonders J, Baker NR (1990) Non-photochemical quenching of F_o in leaves is emission wavelength dependent: consequences for quenching analysis and its interpretation. Photosynth Res **26:** 133–139

Hanson KR, Peterson RB (1985) The stoichiometry of photorespiration during C_3-photosynthesis is not fixed: evidence from combined physical and stereochemical methods. Arch Biochem Biophys **237:** 300–313

Harley PC, Loreto F, Di Marco G, Sharkey TD (1992) Theoretical considerations when estimating the mesophyll conductance to CO_2 flux by analysis of the response of photosynthesis to CO_2. Plant Physiol **98:** 1429–1436

Jordan DB, Ogren WL (1984) The CO_2/O_2 specificity of ribulose 1,5-bisphosphate carboxylase/oxygenase. Dependence on ribulose bisphosphate concentration, pH and temperature. Planta **161:** 308–313

Kane HJ, Viil J, Entsch B, Paul K, Morell MK, Andrews TJ (1994) An improved method for measuring CO_2/O_2 specificity of ribulose bisphosphate carboxylase-oxygenase. Aust J Plant Physiol **21:** 449–461

Kaye GW, Laby TH (1962) Tables of Physical and Chemical Constants. Longmans, Green & Co, London (Russian translation by House of Physico-Mathematical Literature, Moscow)

Krall JP, Edwards GE (1992) Relationship between PSII activity and CO_2 fixation in leaves. Physiol Plant **86:** 180–187

Laisk A (1970) A model of leaf photosynthesis and photorespiration. *In* I Shetlik, ed, Prediction and Measurement of Photosynthetic Productivity. Centre for Agricultural Publishing and Documentation, Wageningen, The Netherlands, pp 295–306

Laisk A (1977) Kinetics of Photosynthesis and Photorespiration in C_3 Plants. Nauka, Moscow (in Russian)

Laisk A, Oja V (1972) A mathematical model of leaf photosynthesis and photorespiration. II. Experimental verification. *In* AA Nitchiporovitch, ed, Theoretical Foundations of the Photosynthetic Productivity. Nauka, Moscow, pp 362–368 (in Russian)

Laisk A, Oja V (1976) Adaptation of the photosynthetic apparatus to light profile in the leaf. Fiziol Rast **23:** 445–451 (in Russian)

Laisk A, Oja V, Rahi M (1970) Diffusion resistances as related to the leaf anatomy. Fiziol Rast **17:** 40–48 (in Russian)

Laisk A, Sumberg A (1994) Partitioning of the leaf CO_2 exchange into components using CO_2 exchange and fluorescence measurements. Plant Physiol **106:** 689–695

Lloyd J, Syvertsen JP, Kriedemann PE, Farquhar GD (1992) Low conductances for CO_2 diffusion from stomata to the sites of carboxylation in leaves of woody species. Plant Cell Environ **15:** 873–899

Loreto F, Di Marco G, Tricoli D, Sharkey TD (1994) Measurements of mesophyll conductance, photosynthetic electron transport and alternative electron sinks of field grown wheat leaves. Photosynth Res **41:** 397–403

Loreto F, Harley PC, Di Marco G, Sharkey TD (1992) Estimation of mesophyll conductance to CO_2 flux by three different methods. Plant Physiol **98:** 1437–1443

Mistshenko KP, Ravdel AA (1965) Short Handbook of Physico-Chemical Data. Himia, Moscow (in Russian)

Ogren WL, Bowes G (1971) Ribulose diphosphate carboxylase regulates soybean photorespiration. Nature **230:** 159–160

Öquist G, Chow WS (1992) On the relationship between the quantum yield of PSII electron transport, as determined by Chl fluorescence and the quantum yield of CO_2-dependent O_2 evolution. Photosynth Res **33:** 51–62

Parkhurst D (1994) Diffusion of CO_2 and other gases inside leaves. New Phytol **126:** 449–479

Parkinson KJ, Penman HL (1970) A possible source of error in the estimation of stomatal resistance. J Exp Bot **21:** 405–409

Pärnik T (1985) Photorespiratory decarboxylation at different CO_2 concentrations. *In* J Viil, GS Grishina, A Laisk, eds, Kinetics of Photosynthetic Carbon Metabolism in C_3 Plants. Valgus, Tallinn, Estonia, pp 121–124

Peterson RB (1989) Partitioning of noncyclic photosynthetic electron transport to O_2 dependent dissipative processes as probed by fluorescence and CO_2 exchange. Plant Physiol **90:** 1322–1328

Peterson RB (1990) Effects of irradiance on the *in vivo* CO_2:O_2 specificity factor in tobacco using simultaneous gas exchange and fluorescence techniques. Plant Physiol **94:** 892–898

Price GD, von Caemmerer S, Evans JR, Jian-Wei Y, Lloyd J, Oja V, Kell P, Harrison K, Gallagher A, Badger M (1994) Specific reduction of chloroplast carbonic anhydrase activity by antisense RNA in transgenic tobacco plants has a minor effect on photosynthetic CO_2 assimilation. Planta **193:** 331–340

Robinson JM (1988) Does O_2 photoreduction occur within chloroplasts in vivo? Physiol Plant **72:** 666–680

Seaton GGR, Walker DA (1990) Chl fluorescence as a measure of photosynthetic carbon assimilation. Proc R Soc Lond B Biol Sci **242:** 29–35

Sumberg A, Laisk A (1996) Measurements of the CO_2/O_2 specificity of ribulose-1,5 bisphosphate carboxylase-oxygenase in leaves. *In* P Mathis, ed, Photosynthesis: From Light to Biosphere, Vol V. Kluwer, Dordrecht, The Netherlands, pp 615–618

Syvertsen JP, Lloyd J, McConchie C, Kriedemann PE, Farquhar GD (1995) On the relationship between leaf anatomy and CO_2 diffusion through the mesophyll of hypostomatous leaves. Plant Cell Environ **18:** 149–157

von Caemmerer S, Evans JR (1991) Determination of the CO_2 pressure in chloroplasts from leaves of several C_3 plants. Aust J Plant Physiol **18:** 287–305

von Caemmerer S, Farquhar GD (1981) Some relationships between the biochemistry of photosynthesis and the gas exchange of leaves. Planta **153:** 376–387